Environmental Science & Technology

Article

pubs.acs.org/est

Changes in Droplet Surface Tension Affect the Observed Hygroscopicity of Photochemically Aged Biomass Burning Aerosol

Michael R. Giordano,[†,‡] Daniel Z. Short,[†,‡] Seyedehsan Hosseini,[‡,§] William Lichtenberg,[†] and Akua A. Asa-Awuku*[,†,‡]

[†]Department of Chemical and Environmental Engineering, University of California—Riverside, Riverside, California United States

[‡]College of Engineering—Center for Environmental Research and Technology (CE-CERT), Riverside, California United States

[§]Department of Mechanical Engineering, University of California—Riverside, Riverside, California United States

Supporting Information

ABSTRACT: This study examines the hygroscopic and surface tension properties as a function of photochemical aging of the aerosol emissions from biomass burning. Experiments were conducted in a chamber setting at the UC-Riverside Center for Environmental Research and Technology (CE-CERT) Atmospheric Processes Lab using two biomass fuel sources, manzanita and chamise. Cloud condensation nuclei (CCN) measurements and off-line filter sample analysis were conducted. The water-soluble organic carbon content and surface tension of the extracted filter samples were measured. Surface tension information was then examined with Köhler theory analysis to calculate the hygroscopicity parameter, κ. Laboratory measurement of biomass burning smoke from two chaparral fuels is shown to depress the surface tension of water by 30% or more at organic matter concentrations relevant at droplet activation. Accounting for surface tension depression can lower the calculated κ by a factor of 2. This work provides evidence for surface tension depression in an important aerosol system and may provide closure for differing sub- and supersaturated κ measurements.

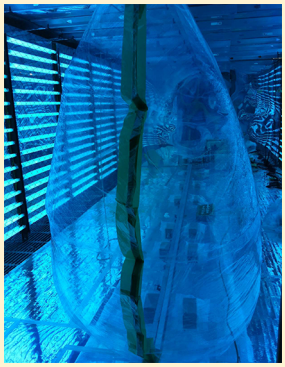

1. INTRODUCTION

Biomass burning can generate significant amounts of aerosol (2−3 Pg yr^{-1}).[1−4] The aerosol formed during burning events has the ability to modify cloud properties[5] and indirectly impact climate radiative forcing.[6,7] Given the significant contribution of biomass burning emissions to the organic aerosol budget, further constraining their hygroscopicity in global models will help reduce uncertainty in simulated aerosol indirect forcing.[6]

Previous works have investigated the cloud condensation nuclei (CCN) properties of biomass burning aerosol. The hygroscopicity of biomass smoke, as represented by the single hygroscopicity parameter κ, has shown a range of values. Much of the variation can be linked to differences in fuels and in burn conditions (e.g. but not limited to refs 8 and 9). The studies range from field measurements to controlled laboratory studies (online and offline measurements). The variation is partly due to the complex aerosol chemistry from different fuel types and the impact of photochemical aging (e.g., refs 10 and 11). Petters et al.[9] measured the CCN activity of 24 biomass fuels (hard and soft woods, shrubs, and grasses); the aerosol ranged from weakly hygroscopic ($\kappa \sim 0.06$) to strongly hygroscopic ($\kappa \sim 0.7$). Novakov and Corrigan[12] concluded that the water-soluble organic species from biomass burning are primarily responsible for their CCN activity. Although, recent research suggests inorganic species may also be important if present in enough concentration.[13,14] Furthermore, primary emissions of biomass burning aerosol can produce additional secondary organic aerosol (SOA) (i.e., refs 15−18). Engelhart et al.[19] measured changes in fresh and aged CCN activity of 12 different fuels (hard and soft woods, shrubs, and grasses) and concluded that decreases in activation were driven by the photochemical production of SOA and the CCN activity of the 12 fuels converged to similar hygroscopicity values ($\kappa \sim 0.2 \pm 0.1$) after a few hours of photochemical processing. Dusek et al.[20] analyzed the subsaturated and supersaturated hygroscopicity of four (2 hard and 2 soft) wood fuels. The hygroscopicity of the smoke from the wood was similar to those reported by Petters et al.,[9] $0.2 > \kappa > 0.05$. However, the supersaturated (CCN derived) hygroscopicity of small particles (50 nm) was twice that of subsaturated (H-TDMA) measurements. The authors concluded that the discrepancy was partially due to surface tension effects that can lead to an overprediction of particle hygroscopicity from CCN measurements;[20] without accounting for surface tension, the true hygroscopicity of the solute composition is not well understood.

Surface active material may be present in atmospheric aerosol. Ruehl et al.[21] found strong evidence that surface tension reduction can occur in microscopic droplets. This surface tension reduction could therefore augment the hygroscopicity of CCN active particles. However, online

Received: April 27, 2013
Revised: August 9, 2013
Accepted: August 19, 2013
Published: August 19, 2013

 © 2013 American Chemical Society

experimental evidence of surface tension depression in microscopic droplets has remained elusive.

Previous work has shown that the composition of the aerosols from biomass burning has a large impact both on hygroscopicity and surface tension. The majority of biomass burning aerosol particulate mass is carbonaceous material.[22,23] Both the primary and secondary carbonaceous components contain complex material called HUmic-LIke Substances (HULIS). HULIS contains slightly soluble substances (mainly dicarboxylic acids) that have been shown to be surface active, range in densities, and modify hygroscopicity and CCN activity (e.g., but not limited to, refs 24−27). HULIS has been isolated from river samples, derived from mimics, and/or extracted from biomass burning filter studies; yet again, CCN derived hygroscopicity has varied from $0.06 < \kappa < 0.34$.[24,26,28−30] X-ray microscopy and spectroscopy has also confirmed HULIS in biomass burning tar balls.[31] To the best of our knowledge, the existence of strong surfactants and HULIS in biomass burning aerosol has been mostly garnered from filter extracts. Field measurements and chamber CCN studies have assumed negligible surface tension depression in supersaturated regimes.

In this work, we use a semicontinuous method to measure surfactant properties and the CCN activity of biomass burning aerosol as it ages with photochemistry. We provide evidence to support the existence of surfactants as well as evidence that photochemical aging can modify aerosol surface tension. We then discuss the importance of surfactants to the CCN ability of these aerosols. Köhler theory analysis is performed to demonstrate the effects of including or excluding surface tension in CCN κ calculations. We also discuss how the variation in biomass burning hygroscopicity can be attributed to the evolution of the surface active material.

2. THEORY FOR CCN ACTIVATION

The theoretical framework of CCN ability can be described by classical Köhler theory.[32] Extensions of Köhler theory have parametrized relationships between critical supersaturation and particle dry diameter. κ-Köhler theory[33] has become a common method of reporting CCN ability and estimating particle hygroscopicity. It has an empirical grounding, is easily understood and translated in both subsaturated and supersaturated regimes, and has a large body of published values.

2.1. Köhler Theory and Single Parameter Hygroscopicity, κ. Köhler theory calculates the saturation ratio, S, over an aqueous droplet as follows:

$$S = a_w \exp\left(\frac{4\sigma_{s/a} M_w}{RT\rho_w D}\right) \tag{1}$$

where a_w is the activity of water in solution, ρ_w is the density of water, M_w is the molecular weight of water, $\sigma_{s/a}$ is the surface tension of the solution/air interface, R is the universal gas constant, T is the temperature, and D is the wet diameter of the droplet.

A single parameter, κ, can parametrize hygroscopicity:[33]

$$\kappa = \frac{4A^3}{27D_d^3 \ln^2 s_c}; \quad \text{where} \quad A = \frac{4\sigma_{s/a} M_w}{RT\rho_w} \tag{2}$$

where D_d is the dry particle diameter, and s_c is the critical supersaturation required to activate a particle with size D_d. D_d is the measured mobility diameter that is calculated as the 50% efficiency for which half of all particles activate at s_c, the instrument supersaturation. From eq 2, κ is interpolated using a linear regression of experimental D_d and calibrated s_c.

κ-Köhler theory works well for ideal droplet water activity conditions, when the growing cloud droplet exists as an aqueous solution and all available solute is dissolved. κ-Köhler theory also applies the ideal surface tension of water, $\sigma_{s/a} = 0.072\ \mathrm{J\ m^{-2}}$. This approximation may not be applicable in the presence of strong surface active compounds.

For completely soluble CCN, s_c scales with $D_d^{-3/2}$. This relationship changes if an aerosol exhibits limited solubility.[34,35] At a characteristic dry diameter of a slightly soluble aerosol, d^*, if $D_d < d^*$ then the amount of water available at the activation point is insufficient to dissolve all solute (changing the s_c-d dependence) and if $D_d > d^*$ then there is sufficient water to dissolve all solute (s_c scales with $D_d^{-3/2}$). The solubility limit of the solute therefore corresponds to $D_d = d^*$ and can be calculated. At the point of complete dissolution, the mass of dissolved solute in the aerosol is

$$m = \frac{\pi}{6}\varepsilon_s \rho_s d^{*3} \tag{3}$$

where ε_s and ρ_s are the volume fraction and density of solute, respectively. Applying Köhler theory, the droplet volume at critical diameter (V_d) can be calculated. If assumed to be approximately equal to the volume of water in the activated droplet, C_{eq} is estimated as follows:[35]

$$C_{eq} = \frac{27}{8}\varepsilon_s \frac{\rho_s}{\rho_w} \frac{d^{*3} s_c^{*3}}{A^3} \tag{4}$$

C_{eq} is used to calculate the average concentration of organic solute at activation and the amount of solute for effective surface tension depression.

2.2. Surface Tension. The Szyszkowski−Langmuir (S-L) equation (eq 5) is used to empirically fit the data over a range of concentrations.[36]

$$\sigma_{s/a} = \sigma_o - \alpha T^* \ln(1 + \beta C) \tag{5}$$

where σ_o is the reference surface tension of pure water, T the temperature in K, C is the water-soluble organic concentration, and α and β are the maximum adsorption density and Langmuir equilibrium adsorption constant, respectively. The latter two variables are calculated with linearly regressed fits of experimental data. Supporting Information (SI) Table S1 shows the α and β parameters of eq 5 as a function of water-soluble organic matter (WSOM). For each s_c-D_d, $\sigma_{s/a}$ at activation is computed iteratively by optimizing the relationships between the Kelvin term, A, concentration at activation C_{eq} (eq 4), and the eq 5 parameters α and β. Additional information about the method can be found in Padró et al.[35]

Due to the different assumptions κ can be calculated under, subscripts are used to clarify the discussion. $\kappa_{apparent}$ refers to a κ-value assuming $\sigma_{s/a} = \sigma_o$. κ_{st} refers to a surface tension corrected hygroscopicity value calculated by assuming a soluble solute with constant surface tension depression. κ_{corr} refers to a surface tension corrected hygroscopicity value calculated by assuming a soluble solute with surface tension depression of the applied eq 5 fit within the same 1−2 h of filter measurement.

3. EXPERIMENTAL METHODS AND INSTRUMENTATION

A series of biomass burning experiments were carried out at the University of California, Riverside College of Engineering,

Center for Environmental Research and Technology (UCR CE-CERT) atmospheric processes lab from summer 2011 to spring 2012. Chamise (*Adenostoma fasciculatum*) and manzanita (*Arctostaphylos glandulosa*), shrubs common to the California chaparral biome, were burned in a wood-burning stove. Both chamise and manzanita were collected in the San Bernardino National Forest (approximately 33.84°, −116.88° and the surrounding area). The collection site is approximately 3600−3900 feet in elevation. Chaparral species such as chamise, manzanita, scrub oak, and ceanothus surround the area. Both manzanita and chamise burned in the flaming regime. The flame integrated modified combustion efficiencies (MCE) of both fuels were greater than 0.98 (where MCE $\equiv (\Delta CO_2)/(\Delta CO_2 + \Delta CO)$.[37]

The smoke was diluted first with an injection system then with a Venturi tube and injected into a 12 m^3 Teflon chamber with final concentration of 50−100 $\mu g\ m^{-3}$. The chamber concentration is within range of ambient and plume-like concentrations also used in previous chamber studies.[15] The sample was injected with a 10:1 total to sample flow ratio. As short of a copper transfer line as possible was used for the smoke injection, approximately 7 m in length. The enclosure is surrounded by 170 ultraviolet (UV) lights with peak intensity of 350 nm (350 BL, Sylvania). UV lights were turned on 1 h after injection to promote photochemistry and remained on until the experiment concluded. The chamber was flushed and filled with filtered air prior to injection. The temperature of the chamber ranged approximately from 20 to 27 °C during the experiment.

The experiment was operated until the chamber was empty (up to 6 h). Chemical aging was monitored with Teledyne carbon monoxide (CO) and ozone (O_3) gas analyzers and suggested realistic aging occurred in the chamber (see SI Figure S1). Previous studies have used similar measurements to monitor plume age in ambient studies. Yokelson et al.[17] reported $\Delta O_3/\Delta CO \approx 0.25$ for a 1.5 h old plume in the Yucatan. The chamber aging process is similar for manzanita; the $\Delta O_3/\Delta CO = 0.20$ after 1.5 h of irradiation. $\Delta O_3/\Delta CO$ steadily increased to 0.5. For chamise, $\Delta O_3/\Delta CO$ also displayed a steady rise though it was delayed for a number of hours. Chamise had an order of magnitude greater formation of O_3 than manzanita, leading to a $\Delta O_3/\Delta CO > 6.0$ at the end of the experiment. The comparison of chamber $\Delta O_3/\Delta CO$ data with field measurements suggests that realistic aging can be achieved in the chamber system.

Scanning Mobility CCN Analysis (SMCA)[38] was used to obtain fast size-resolved CCN activity of the aging system. The sampled aerosol was size-classified using a Scanning Mobility Particle Sizer (SMPS, TSI 3080/3081). The monodisperse stream from the classifier was split, and one stream entered a condensation particle counter (TSI 3772) while the other stream was sampled with a DMT Continuous Flow Streamwise Thermal Gradient Chamber CCN counter (CCNC).[39,40] The CCNC instrument was operated at a 10:1 sheath-to-aerosol ratio with a sample flow of 0.5 L min^{-1}. The total concentration (CN) of sized particles measured by the CPC determined the ratio of CCN/CN. For each supersaturation, s_c, the activation diameter, D_d, was defined as the diameter for which CCN/CN = 0.5. The experimental setup was calibrated with ammonium sulfate ($(NH_4)_2SO_4$) aerosol. CCNC calibration information is provided in Supporting Information (Table S2).

Teflon filter samples were taken during lights off (the first hour of the experiment) and lights on (the remainder of the experiment). For offline analysis, the filters were sonicated in Millipore DI water (18 mΩ, TOC ∼ 3 ppb) for 1 h. The aqueous extracts were then filtered using a Whatman 25 mm syringe filter to remove large nondissolved particles. Then, samples were diluted into 10 mL DI water at ratios of 1:3, 1:4, 1:5, and 1:6. The surface tension of each sample was then measured with a pendant drop tensiometer (Attension Theta 200, Biolin Scientific, Sweden). The optical tensiometer captures at least 100 images of the droplet and computes droplet surface tension through application of the Young−Laplace equation;[41,42] the standard deviations for $\sigma_{s/a}$ are less than 0.05 mN m^{-1} for a given sample at one concentration. The water-soluble organic carbon (WSOC) concentrations of each sample were measured using a Total Organic Carbon analyzer (Sievers 900, GE). The error associated with TOC measurements is ±2%. Organic carbon (OC) concentration (taken as WSOC here) was converted to organic mass (OM) concentration using an OM/OC measurement from an Aerodyne High-Resolution Particle Time-of-Flight Aerosol Mass Spectrometer (HR-PToF AMS)[43] connected directly to the environmental chamber. OM/OC values were 1.46 ± 0.064 and 1.41 ± 0.057 for chamise and manzanita, respectively.

4. RESULTS

In both fuel species, photochemistry modifies the presence of surface active material found in biomass burning aerosol. This work shows that surface active materials are present in aerosol generated from chamber biomass burning experiments. The effective surface tension depression, $((\sigma_o - \sigma_{s/a})/\sigma_o) \times 100$, is plotted as a function of the concentration of water-soluble organic carbon (Figure 1). Up to 30% surface tension depression is observed from the filter extracts. The surface tension depression from filter extracts is consistent with previous works. Asa-Awuku et al.[24] observed biomass burning extract samples that exhibited a surface tension depression of nearly 20% at their measured concentration. Salma et al.[44] found up to 30% surface tension depression from atmospheric humic-like substances. Kiss et al.[27] showed that HULIS extracts of atmospheric aerosols depressed surface tension by up to 42%. Facchini et al.[45] reported that polyacidic compounds from aerosols, as HULIS are, depressed surface tension by nearly 25%. The surface tension data and WSOC data is fit to the Szyszkowski−Langmuir (S-L) equation. Chamise aerosol sampled in the dark chamber is less surface active than aerosol sampled after two and four hours of photochemistry (Figure 1). Conversely, manzanita aerosol displays the opposite trend. Manzanita aerosol irradiated for five hours is less surface active than aerosol sampled from a dark chamber, with intermediate stages that are only slightly less active than nonaged particles (Figure 1).

The CCN activity is also modified by photochemistry. s_c-D_d pairs for chamise and manzanita are shown in Figure 2 (where s_c is the critical supersaturation at which a particle activates). The critical diameter, D_d, required for activation at a given s can span 50 nm during a 4 h photochemical experiment. Freshly emitted aerosol appears to be hygroscopic; D_d for chamise and manzanita can be greater or equal to $\kappa = 0.4$. The greatest variability in D_d for both fuel types occurs at lower instrument s of 0.25% and 0.46%. The average best fit $\kappa_{apparent}$ is 0.098 ± 0.001 and 0.238 ± 0.001 for chamise and manzanita, respectively. Petters et al.[9] reported a κ of 0.10 for manzanita branches from a stack burn. This differs from our average value of 0.238 from the environmental chamber burn study of

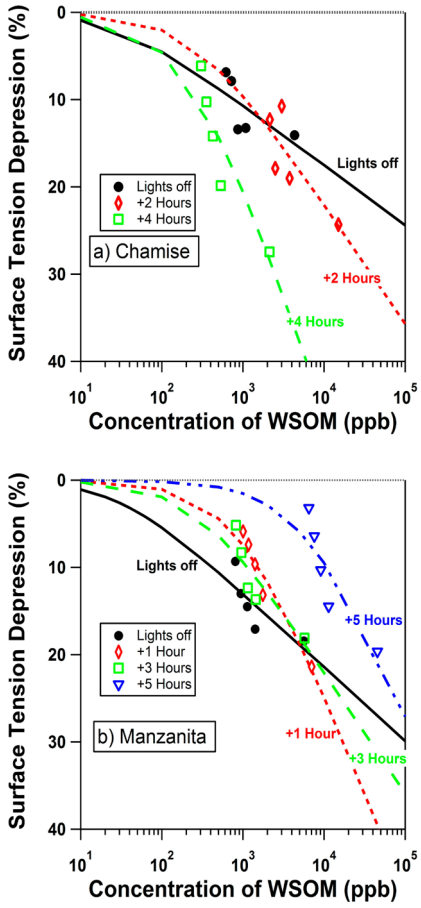

Figure 1. Szyskowski–Langmuir fits and data for chamise (a) and manzanita (b) biomass burning aerosol. Surface tension depression vs water-soluble organic matter concentration is shown as a function of time of irradiation. The fit parameters α and β are given in SI Table S1.

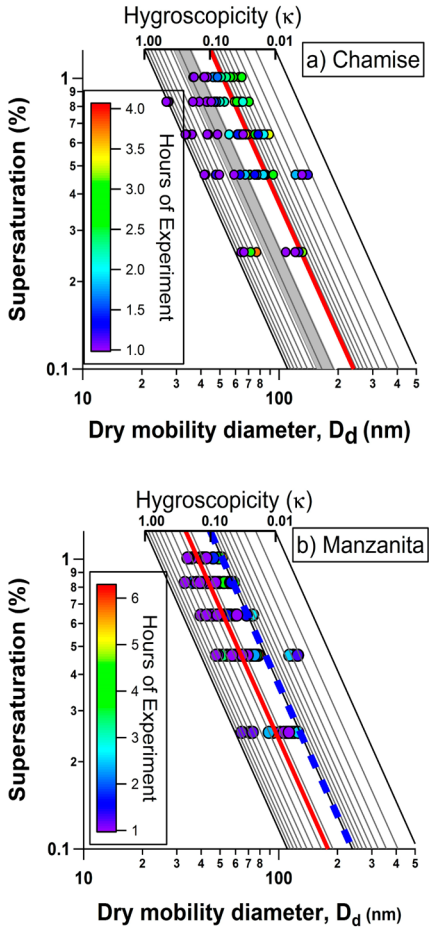

Figure 2. CCN activity of biomass burning aerosol from chamise (a) and manzanita (b). Data from a dark chamber are colored purple while irradiated data follows the color scale shown. The best-fit line of the data is represented in red for both graphs. The shaded region in part a is the reported average data from Engelhart et al.[19] The blue line in Figure 2b is the reported data from Petters et al.[9]

manzanita branches and leaves. Additionally, Petters et al.[9] note that manzanita is a species that is well characterized by a range $0.05 < \kappa < 0.19$. From Figure 2, it can be seen that for the majority of the experiment our measurements fall within this range. This is especially true of photochemically aged measurements. Our nonphotochemically aged CCN measurements have higher average $\kappa_{apparent}$ values.

For chamise, Petters et al.[9] reported a wide range of κ values for stack burns of chamise, $\sim 0.2 < \kappa < 0.5$, and also for chamber burns, $\sim 0.2 < \kappa < 0.35$. Engelhart et al.[19] reported a similar range for primary emissions of chamise, approximately $0.3 < \kappa < 0.5$, and for oxidized emissions, $0.15 < \kappa < 0.25$, reported at two different supersaturations. Our reported values are in line with both of these measurements (e.g., photochemical aging driving $\kappa_{apparent}$ values down (Figure 2)). Our lower bound $\kappa_{apparent}$ value is lower than both Petters et al.[9] and Engelhart et al.[19] The discrepancy may be due to fuel condition (water content) upon burning or fire conditions (e.g., MCE).[8] It is noted that wood-stove burning can result in higher MCE than open burning. Petters et al.[9] reported 5–10 min of flaming followed by 5–10 min of smoldering as compared to our consistently flaming phase for injection of the smoke into the smog chamber. Engelhart et al.[19, reported in 15] reported a MCE of 0.94, compared to our MCE > 0.98. Comparisons of $\kappa_{apparent}$ biomass species suggest differing amounts of hygroscopic material are produced during burns of the same fuel.

The average reported $\kappa_{apparent}$ is sensitive to changes in surface tension. In Table 1, the overall average κ_{st} and A_{st} are calculated for the corresponding data in Figure 2 by applying constant values for $\sigma_{s/a}$. The average κ_{st} can be ≤ 0.1 for a 25% surface tension depression (Table 1). $\kappa_{st} \leq 0.1$ is similar to subsaturated H-TDMA measurements of biomass burning aerosol.[20,46]

Table 1. Sensitivity of A (Kelvin Term) and κ Values Using the Data in Figure 2 Calculated with Varying Degrees of Constant Surface Tension Depression

	surface tension depression					
	0%	5%	10%	15%	20%	25%
A, Kelvin term	2.091	1.987	1.882	1.778	1.673	1.568
κ_{st} (chamise)	0.265	0.227	0.193	0.162	0.135	0.112
κ_{st} (manzanita)	0.226	0.194	0.165	0.139	0.116	0.095

Figure 3 shows both $\kappa_{apparent}$ and κ_{corr} for manzanita and chamise aerosol as a function of time. Both fuels show dependence of hygroscopicity with photochemistry; $\kappa_{apparent}$ before irradiation is higher than after photochemistry for both manzanita and chamise. Both species decrease $\kappa_{apparent}$ by a factor of 2 or more with photochemical activity (Figure 3).

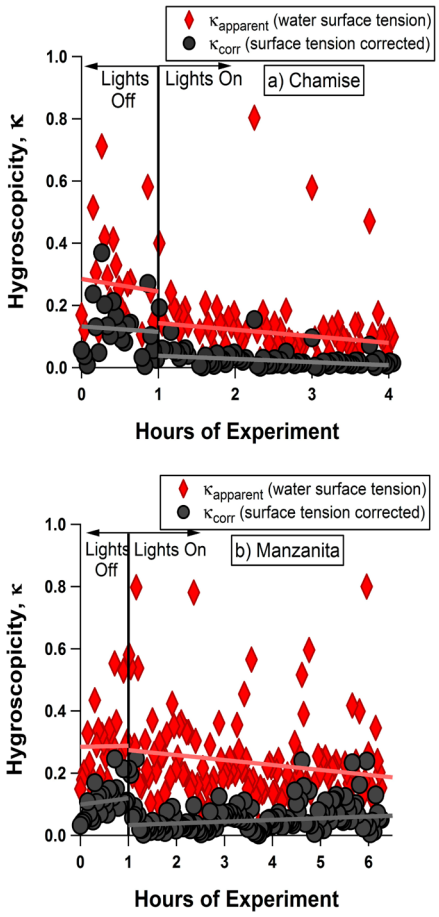

Figure 3. Single parameter hygroscopicity, κ, calculated without ($\kappa_{apparent}$) and with (κ_{corr}) surface tension correction for chamise (top, A) and manzanita (bottom, B). Solid vertical lines indicate when lights are turned on, 1 h after injection. A 7-min running average of the data before and after lights-on is also provided.

$\kappa_{apparent}$ for chamise is 0.21 ± 0.11 in the dark and an average of 0.09 ± 0.06 after irradiation. For manzanita, $\kappa_{apparent}$ is 0.33 ± 0.11 in the dark and an average of 0.12 ± 0.04 after irradiation. Stronger surfactants (indicative of HULIS) are present during the aging of chamise aerosol (Figure 1). As a result, κ_{corr} decreases. The changes in surface activity could be due to the chemical processing of HULIS during photochemical aging.

κ_{corr} values of chamise aerosol indicate the composition of aerosol ranges from slightly soluble to wettable and insoluble. If $\sigma_{s/a}$ is accounted for, the κ_{corr} for chamise becomes 0.10 ± 0.06 in the dark and reduces to an average κ_{corr} 0.02 ± 0.02 (Figure 3a) during aging. The change in κ_{corr} is comparable for manzanita, where κ_{corr} is 0.12 ± 0.05 in the dark and reduces to an average κ_{corr} 0.06 ± 0.04 after lights on (Figure 3b). In the case of manzanita, the presence of surfactants decreases with photochemical aging (Figure 1). κ_{corr} indicates that the aerosol solute from both fuels becomes less hygroscopic with aging.

The results presented here support the growing body of evidence that surface active materials are present in biomass burning emissions. The surfactant effects are real and can be observed from semicontinuous measurements of offline filter extracts of environmental chamber aerosol. The aerosol formed from the combustion of chamise and manzanita is able to depress droplet surface tension up to 30% at concentrations relevant for droplet activation. Köhler theory when combined with measurements of surface tension, solubility, and CCN activity can aid our understanding of organic solute hygroscopicity. The inclusion of surfactant parameters is in agreement and consistent with findings that show that the organic component of the aerosol has soluble properties with a κ hygroscopicity parameter of ≤ 0.1. In both cases, aging of the primary aerosol produces less hygroscopic material.

The majority of aerosol formed in these experiments is organic (SI Figure S2). The presence of nitrates, sulfates, and other inorganic salts from wild fire events could potentially induce surface tension salting out effects.[24] This would likely increase soluble material and $\kappa_{apparent}$ values. However, only 5% of the total aerosol needs to be surface active for closure of sub- and supersaturated hygroscopicity measurements to disagree.[20] Surface tension properties in biomass burning systems should be accounted for when estimating hygroscopicity from supersaturated data sets. There are additional factors that can affect both sub- and supersaturated κ, including both fractal dimension (particle shape) and particle composition. However, surface tension has the greatest impact in the supersaturated regime and appears to reconcile the differences in previously reported κ values.

Our analysis confirms that hygroscopicity derived from CCN activity can be overestimated by a factor of 2 if surface tension effects are not accounted. The findings are consistent with the recent work of Martin et al.[46] and Kristenen et al.[28] who found that subsaturated hygroscopicity for biomass burning and HULIS is less than CCN derived values. Semicontinuous surface tension analysis can account for the presence and evolution of surfactants. It may also bridge the gap between subsaturated and supersaturated hygroscopicity measurements. Unifying the two regimes may reduce uncertainties in the prediction of indirect forcing of biomass burning aerosol.

■ ASSOCIATED CONTENT

Ⓢ Supporting Information

Calibration information for the CCNC, fit coefficients for the Szyszkowski−Langmuir equation, AMS composition data, and $\Delta O_3/\Delta CO$ information for both fuels. This material is available free of charge via the Internet at http://pubs.acs.org.

■ AUTHOR INFORMATION

Corresponding Author

*E-mail: akua@engr.ucr.edu.

Notes

The authors declare no competing financial interest.

■ ACKNOWLEDGMENTS

Many thanks to David Weise and Joey Chong of the USDA Forest Service for their advice and pivotal role in the acquisition of fuels. The authors would also like to thank David Cocker and the Keck Foundation for use of the environmental chamber. M.G. and D.S. would like to thank California NASA Space Grant Consortium for partially supporting this work. M.G. and A.A. would also like to thank the U.S. Environmental Protection Agency for funding this work made possible by EPA Grant No. 83504001. S.H. would like to thank W. Miller and the Strategic Environmental Research and Development Program (SERDP) projects SI-1648 and SI-1649. W. Lichtenberg thanks the National Science Foundation (1032388) for undergraduate research support. Any opinions, findings, and conclusions expressed in this material are those of

the authors and do not necessarily reflect the views of NSF, NASA, or EPA.

REFERENCES

(1) van der Werf, G. R.; Randerson, J. T.; Giglio, L.; Collatz, G. J.; Kasibhatla, P. S.; Arellano, A. F., Jr. Interannual variability in global biomass burning emissions from 1997 to 2004. *Atmos. Chem. Phys.* **2006**, *6*, 3423−3441, DOI: 10.5194/acp-6-3423-2006.

(2) Reid, J. S.; Koppmann, R.; Eck, T. F.; Eleuterio, D. P. A review of biomass burning emissions. Part II: Intensive physical properties of biomass burning particles. *Atmos. Chem. Phys.* **2005**, *5*, 799−825, DOI: 10.5194/acp-5-799-2005.

(3) Andreae, M. O.; Rosenfeld, D.; Artaxo, P.; Costa, A. A.; Frank, G. P.; Longo, K. M.; Silva-Dias, M. A. F. Smoking rain clouds over the Amazon. *Science* **2004**, *303*, 1337−1342, DOI: 10.1126/science.1092779.

(4) Crutzen, P. J.; Andreae, M. O. Biomass burning in the tropics: Impact on atmospheric chemistry and biogeochemical cycles. *Science* **1990**, *250*, 1669−1678, DOI: 10.1126/science.250.4988.1669.

(5) Reutter, P.; Su, H.; Trentmann, J.; Simmel, M.; Rose, D.; Gunthe, S. S.; Wernli, H.; Andreae, M. O.; Pöschl, U. Aerosol- and updraft-limited regimes of cloud droplet formation: Influence of particle number, size and hygroscopicity on the activation of cloud condensation nuclei (CCN). *Atmos. Chem. Phys.* **2009**, *9*, 7067−7080, DOI: 10.5194/acp-9-7067-2009.

(6) Liu, X.; Wang, J. How important is organic aerosol hygroscopicity to aerosol indirect forcing? *Environ. Res. Lett.* **2010**, *5* (4), DOI: 10.1088/1748-9326/5/4/044010.

(7) *Climate Change 2007: The Physical Science Basis. Contribution of Working Group I to the Fourth Assessment Report of the Intergovernmental Panel on Climate Change*; Intergovernmental Panel on Climate Change: Geneva, Switzerland, 2007.

(8) Carrico, C. M.; Petters, M. D.; Kreidenweis, S. M.; Sullivan, A. P.; McMeeking, G. R.; Levin, E. J. T.; Engling, G.; Malm, W. C.; Collett, J. L. Water uptake and chemical composition of fresh aerosols generated in open burning of biomass. *Atmos. Chem. Phys.* **2010**, *10*, 5165−5178, DOI: 10.5194/acp-10-5165-2010.

(9) Petters, M. D.; Carrico, C. M.; Kreidenweis, S. M.; Prenni, A. J.; DeMott, P. J.; Collett, J. L.; Moosmüller, H. Cloud condensation nucleation activity of biomass burning aerosol. *J. Geophys. Res.* **2009**, *114*, D22205 DOI: 10.1029/2009JD012353.

(10) DeCarlo, P. F.; Ulbrich, I. M.; Crounse, J.; de Foy, B.; Dunlea, E. J.; Aiken, A. C.; Knapp, D.; Weinheimer, A. J.; Campos, T.; Wennberg, P. O.; Jimenez, J. L. Investigation of the sources and processing of organic aerosol over the Central Mexican Plateau from aircraft measurements during MILAGRO. *Atmos. Chem. Phys.* **2010**, *10*, 5257−5280, DOI: 10.5194/acp-10-5257-2010.

(11) Janhäll, S.; Andreae, M. O.; Pöschl, U. Biomass burning aerosol emissions from vegetation fires: Particle number and mass emission factors and size distributions. *Atmos. Chem. Phys.* **2010**, *10*, 1427−1439, DOI: 10.5194/acp-10-1427-2010.

(12) Novakov, T.; Corrigan, C. E. Cloud condensation nucleus activity of the organic component of biomass smoke particles. *Geophys. Res. Lett.* **1996**, *23*, 2141−2144, DOI: 10.1029/96GL01971.

(13) Hand, J. L.; Malm, W. C.; Laskin, A.; Day, D.; Lee, T.; Wang, C.; Carrico, C.; Carrillo, J.; Cowin, J. P.; Collett, J.; Iedema, M. J. Optical, physical, and chemical properties of tar balls observed during the Yosemite aerosol characterization study. *J. Geophys. Res.: Atmos.* **2005**, *110* (D21), DOI: 10.1029/2004JD005728.

(14) Levin, E. J. T.; McMeeking, G. R.; Carrico, C. M.; Mack, L. E.; Kreidenweis, S. M.; Wold, C. E.; Moosmüller, H.; Arnott, W. P.; Hao, W. M.; Collett, J. L.; Malm, W. C. Biomass burning smoke aerosol properties measured during fire laboratory at Missoula experiments (FLAME). *J. Geophys. Res.: Atmos.* **2010**, *115* (D18), DOI: 10.1029/2009JD013601.

(15) Hennigan, C. J.; Miracolo, M. A.; Engelhart, G. J.; May, A. A.; Presto, A. A.; Lee, T.; Sullivan, A. P.; McMeeking, G. R.; Coe, H.; Wold, C. E.; Hao, W.-M.; Gilman, J. B.; Kuster, W. C.; de Gouw, J.; Schichtel, B. A.; Collett, J. L.; Kreidenweis, S. M.; Robinson, A. L. Chemical and physical transformations of organic aerosol from the photo-oxidation of open biomass burning emissions in an environmental chamber. *Atmos. Chem. Phys.* **2011**, *11*, 7669−7686, DOI: 10.5194/acp-11-7669-2011.

(16) de Gouw, J.; Jimenez, J. L. Organic aerosols in the Earth's atmosphere. *Environ. Sci. Technol.* **2009**, *43*, 7614−7618, DOI: 10.1021/es9006004.

(17) Yokelson, R. J.; Crounse, J. D.; DeCarlo, P. F.; Karl, T.; Urbanski, S.; Atlas, E.; Campos, T.; Shinozuka, Y.; Kapustin, V.; Clarke, A. D.; Weinheimer, A.; Knapp, D. J.; Montzka, D. D.; Holloway, J.; Weibring, P.; Flocke, F.; Zheng, W.; Toohey, D.; Wennberg, P. O.; Wiedinmyer, C.; Mauldin, L.; Fried, A.; Richter, D.; Walega, J.; Jimenez, J. L.; Adachi, K.; Buseck, P. R.; Hall, S. R.; Shetter, R. Emissions from biomass burning in the Yucatan. *Atmos. Chem. Phys.* **2009**, *9*, 5785−5812, DOI: 10.5194/acp-9-5785-2009.

(18) Eatough, D. J.; Eatough, N. L.; Pang, Y.; Sizemore, S.; Kirchstetter, T. W.; Novakov, T.; Hobbs, P. V. Semi volatile particulate organic material in southern Africa during SAFARI 2000. *J. Geophys. Res.* **2003**, *108* (D13), 8479 DOI: 10.1029/2002JD002296.

(19) Engelhart, G. J.; Hennigan, C. J.; Miracolo, M. A.; Robinson, A. L.; Pandis, S. N. Cloud condensation nuclei activity of fresh primary and aged biomass burning aerosol. *Atmos. Chem. Phys.* **2012**, *12*, 7285−7293, DOI: 10.5194/acp-12-7285-2012.

(20) Dusek, U.; Frank, G. P.; Massling, A.; Zeromskiene, K.; Iinuma, Y.; Schmid, O.; Helas, G.; Hennig, T.; Wiedensohler, A.; Andreae, M. O. Water uptake by biomass burning aerosol at sub- and supersaturated conditions: Closure studies and implications for the role of organics. *Atmos. Chem. Phys.* **2011**, *11*, 9519−9532, DOI: 10.5194/acp-11-9519-2011.

(21) Ruehl, C. R.; Chuang, P. Y.; Nenes, A.; Cappa, C. D.; Kolesar, K. R.; Goldstein, A. H. Strong evidence of surface tension reduction in microscopic aqueous droplets. *Geophys. Res. Lett.* **2012**, *39* (23), DOI: 10.1029/2012GL053706.

(22) Decesari, D.; Fuzzi, S.; Facchini, M. C.; Mircea, M.; Emblico, L.; Cavalli, F.; Maenhaut, W.; Chi, X.; Schkolnik, G.; Falkovich, A.; Rudich, Y.; Claeys, M.; Pashynska, V.; Vas, G.; Kourtchev, I.; Vermeylen, R.; Hoffer, A.; Andreae, M. O.; Tagliavini, E.; Moretti, F.; Artaxo, P. Characterization of the organic composition of aerosols from Rondonia, Brazil, during the LBA-SMOCC 2002 experiment and its representation through model compounds. *Atmos. Chem. Phys.* **2006**, *6*, 375−402, DOI: 10.5194/acp-6-375-2006.

(23) Artaxo, P.; Martins, J. V.; Yamasoe, M. A.; Procopio, A. S.; Pauliquevis, T. M.; Andreae, M. O.; Guyon, P.; Gatti, L. V.; Leal, A. M. C. Physical and chemical properties of aerosols in the wet and dry seasons in Rondonia, Amazonia. *J. Geophys. Res.: Atmos.* **2002**, *107* (D20), 8081 DOI: 10.1029:2001JD000666.

(24) Asa-Awuku, A.; Sullivan, A. P.; Hennigan, C. J.; Weber, R. J.; Nenes, A. Investigation of molar volume and surfactant characteristics of water-soluble organic compounds in biomass burning aerosol. *Atmos. Chem. Phys.* **2008**, *8*, 799−812, DOI: 10.5194/acp-8-799-2008.

(25) Dinar, E.; Taraniuk, I.; Graber, E. R.; Katsman, S.; Moise, T.; Anttila, T.; Mentel, T. F.; Rudich, Y. Cloud condensation nuclei properties of model and atmospheric HULIS. *Atmos. Chem. Phys.* **2006**, *6*, 2465−2481, DOI: 10.5194/acp-6-2465-2006.

(26) Dinar, E.; Mentel, T. F.; Rudich, Y. The density of humic acids and humic-like substances (HULIS) from fresh and aged wood burning and pollution aerosol particles. *Atmos. Chem. Phys.* **2006b**, *6*, 5213−5224, DOI: 10.5194/acp-6-5213-2006.

(27) Kiss, G.; Tombácz, E.; Hansson, H.-C. Surface tension effects of humic-like substances in the aqueous extract of tropospheric fine aerosol. *J. Atmos. Chem.* **2005**, *50* (3), 279−294.

(28) Kristensen, T. B.; Wex, H.; Nekat, B.; Nøjgaard, J. K.; Pinxteren, D.; Lowenthal, D. H.; Mazzoleni, L. R.; Dieckmann, K.; Koch, C. B.; Mentel, T. F.; Herrmann, H.; Hallar, A. G.; Stratmann, F.; Bilde, M. Hygroscopic growth and CCN activity of HULIS from different environments. *J. Geophys. Res.: Atmos.* **2012**, *117* (D22), DOI: 10.1029/2012JD018249.

(29) Fors, E. O.; Rissler, J.; Massling, A.; Svenningsson, B.; Andreae, M. O.; Dusek, U.; Frank, G. P.; Hoffer, A.; Bilde, M.; Kiss, G.; Janitsek,

S.; Henning, S.; Facchini, M. C.; Decesari, S.; Swietlicki, E. Hygroscopic properties of Amazonian biomass burning and European background HULIS and investigation of their effects on surface tension with two models linking H-TDMA to CCNC data. *Atmos. Chem. Phys.* **2010**, *10*, 5625−5639, DOI: 10.5194/acp-10-5625-2010.

(30) Ziese, M.; Wex, H.; Nilsson, E.; Salma, I.; Ocskay, R.; Hennig, T.; Massling, A.; Stratmann, F. Hygroscopic growth and activation of HULIS particles: Experimental data and a new iterative parameterization scheme for complex aerosol particles. *Atmos. Chem. Phys.* **2008**, *8*, 1855−1866, DOI: 10.5194/acp-8-1855-2008.

(31) Tivanski, A. V.; Hopkins, R. J.; Tyliszczak, T.; Gilles, M. K. Oxygenated interface on biomass burn tar balls determined by single particle scanning transmission X-ray microscopy. *J. Phys. Chem. A* **2007**, *111* (25), 5448−5458, DOI: 10.1021/jp070155u.

(32) Köhler, H. The nucleus in and the growth of hygroscopic droplets. *Trans. Faraday Soc.* **1936**, *43*, 1152−1161.

(33) Petters, M. D.; Kreidenweis, S. M. A single parameter representation of hygroscopic growth and cloud condensation nucleus activity. *Atmos. Chem. Phys.* **2007**, *7*, 1961−1971, DOI: 10.5194/acp-7-1961-2007.

(34) Petters, M. D.; Kreidenweis, S. M. A single parameter representation of hygroscopic growth and cloud condensation nucleus activity. Part 2: Including solubility. *Atmos. Chem. Phys.* **2008**, *8*, 6273−6279, DOI: 10.5194/acp-8-6273-2008.

(35) Padró, L. T.; Asa-Awuku, A.; Morisson, R.; Nenes, A. Inferring thermodynamic properties from CCN activation experiments: Single-component and binary aerosols. *Atmos. Chem. Phys.* **2007**, *7*, 5263−5274, DOI: 10.5194/acp-7-5263-2007.

(36) Szyskowski, B. V. Experimentelle studien über kapillare eigenschaften der wässerigen lösungen von fettsauren. *Z. Phys. Chem.* **1908**, *64*, 385−414.

(37) Ward, D. E.; Hao, W. M. Projections of emissions from burning of biomass for use in studies of global climate and atmospheric chemistry. *Proceedings of the 84th Annual Meeting and Exhibition Air and Waste Management Association*, Vancouver, British Colombia, Canada, June 16−21, 1991; Vol. *19*

(38) Moore, R. H.; Nenes, A.; Medina, J. Scanning mobility CCN analysis—A method for fast measurements of size-resolved CCN distributions and activation kinetics. *Aerosol Sci. Technol.* **2010**, *44* (10), 861−871, DOI: 10.1080/02786826.2010.498715.

(39) Roberts, G. C.; Nenes, A. A continuous-flow streamwise thermal-gradient CCN chamber for atmospheric measurements. *Aerosol Sci. Technol.* **2005**, *39* (3), 206−221, DOI: 10.1080/027868290913988.

(40) Rose, D.; Gunthe, S. S.; Mikhailov, E.; Frank, G. P.; Dusek, U.; Andreae, M. O.; Pöschl, U. Calibration and measurement uncertainties of a continuous-flow cloud condensation nuclei counter (DMT-CCNC): CCN activation of ammonium sulfate and sodium chloride aerosol particles in theory and experiment. *Atmos. Chem. Phys.* **2008**, *8*, 1153−1179, DOI: 10.5194/acp-8-1153- 2008.

(41) Andreas, J. M.; Hauser, E. A.; Tucker, W. B. Boundary tension by pendant drops. *J. Phys. Chem.* **1937**, *42* (8), 1001−1019, DOI: 10.1021/j100903a002.

(42) Fordham, S. On the calculation of surface tension from measurements of pendant drops. *Proc. R. Soc. Lond. A* **1948**, 194 DOI: 10.1098/rspa.1948.0063.

(43) DeCarlo, P. F.; Kimmel, J. R.; Trimborn, A.; Northway, M. J.; Jayne, J. T.; Aiken, A. C.; Gonin, M.; Fuhrer, K.; Horvath, T.; Docherty, K. S.; Worsnop, D. R.; Jimenez, J. L. Field-deployable, high-resolution, time-of-flight aerosol mass spectrometer. *Anal. Chem.* **2006**, *78* (24), 8281−8289, DOI: 10.1021/ac061249n.

(44) Salma, I.; Ocskay, R.; Varga, I.; Maenhaut, W. Surface tension of atmospheric humic-like substances in connection with relaxation, dilution, and solution pH. *J. Geophys. Res.* **2006**, *111*, D23205 DOI: 10.1029/2005JD007015.

(45) Facchini, M. C.; Decesari, S.; Mircea, M.; Fuzzi, S.; Loglio, G. Surface tension of atmospheric wet aerosol and cloud/fog droplets in relation to their organic carbon content and chemical composition. *Atmos. Environ.* **2000**, *34*, 4853−4857.

(46) Martin, M.; Tritscher, T.; Jurányi, Z.; Heringa, M. F.; Sierau, B.; Weingartner, E.; Chiricob, R.; Gysel, M. S.H.; Prévôt, A. S. H.; Baltenspergerb, U.; Lohmann, U. Hygroscopic properties of fresh and aged wood burning particles. *J. Aerosol Sci.* **2013**, *56*, 15−29, DOI: 10.1016/j.jaerosci.2012.08.006.